Proceedings of the ASME 2008 International Design Engineering Technical Conferences & Computers and Information in Engineering Conference
IDETC/CIE 2008
August 3-6, 2008, Brooklyn, New York, USA

DETC2008-49563

TOPOLOGY OPTIMIZATION OF A MEMS RESONATOR USING HYBRID FUZZY TECHNIQUES

Mohamed S. Senousy
Ph.D. Candidate
Mechanical Engineering Department
The University of British Columbia (UBC),
Vancouver V6T1Z4, Canada
Email: msenousy@mech.ubc.ca

Hesham A. Hegazi
Assistant Professor
Department of Mechanical Engineering
The American University in Cairo (AUC), Cairo 11511, EGYPT
Email: hhegazi@aucegypt.edu

Sayed M. Metwalli
Professor of Machine Design, Fellow ASME
Department of Mechanical Design and Production
Cairo University, Cairo 12316, EGYPT
Email: metwallis2@asme.org

ABSTRACT
This paper introduces a new methodology for the design of structures by geometry and topology optimization accounting for loading and boundary conditions as well as material properties. The Fuzzy Heuristic Gradient Projection (FHGP) method is used as a direct search technique for the geometry optimization, while the Complex Method (CM) is used as a random search technique for the topology optimization. In the proposed method, elements are designed such that they all have the same amount of stresses using the Fuzzy Heuristic Gradient Projection method. On the other hand, the complex method is used for the topology optimization step satisfying any constraint other than the stress constraint. The developed hybrid fuzzy technique is applied for different applications ranging from micro-scale to macro-scale applications. The method is applied to a micro-mechanical resonator as a micro-electro-mechanical system (MEMS). The resonator is solved for minimum weight and is subjected to an equality frequency constraint and an inequality stress constraint. The proposed method is compared with the Multi-objective Genetic Algorithms (MOGAs) on solving the MEMS resonator. Results showed that the proposed hybrid fuzzy technique converges to optimum solutions faster than (MOGAs). The time consumed is improved by a 77%.

KEYWORDS
Topology Optimization, Fuzzy Logic, Fuzzy Heuristic Gradient Projection, Hybrid Fuzzy Techniques

INTRODUCTION

Micro-electromechanical systems (MEMS) are the integration of micro-sensors and actuators that can sense the environment and have the ability to react to changes in that environment with the use of a microcircuit controller. In addition to the microelectronics packaging, MEMS include integrating antenna structures for desired sensing and actuating functions. Micro-components make the system faster, more reliable, cheaper, and capable of incorporating more complex functions. A variety of materials can be used to manufacture MEMS devices, such as crystalline silicon, polycrystalline silicon, and silicon nitride. Therefore, a variety of mechanical microstructures including beams, diaphragms, grooves, orifices, springs, gears, suspensions and a great diversity of other complex mechanical structures has been created (Varadan, Jiang and Varadan, 2001). (Kamalian et al. 2002) developed a synthesis tool for MEMS applying Single-objective Genetic Algorithms (SOGAs) and Multi-objective Genetic Algorithm (MOGAs). A meandering resonator was

solved for a specified natural frequency to compare Genetic Algorithms (GAs) to the optimization technique of Simulated Annealing (SA). The results showed that Simulated Annealing could synthesize valid designs faster than genetic algorithms. The authors, however, argued that simulated annealing couldn't solve for multi-objective problems as Genetic Algorithms do. In addition, they indicated that it is a less robust method for MEMS synthesis problems. Results proved that GA is general, robust, and able to optimize for multi design objectives. (Clark et al. 2002) presented the development of a simulation program (SUGAR) for planar MEMS devices. Nonlinear-coupled differential equations are solved based on the nodal analysis approach, that is, in MEMS device the law of static equilibrium is applied to each node such that the summation of the forces and moments on the nodes are equal to zero. Structural models can relate forces and nodes on each node. A simple MEMS structure was presented to demonstrate the assemblage method. The authors verified their developed program by comparing its results with analytical solutions, experimental data, and FEM simulations. The authors presented the modeling of linear beam, nonlinear beam, and gap with contact forces models. The demonstrated program showed how it was able to handle nonlinearities due to electrostatics and stiffness in many types of planar MEMS devices. Later on (Clark et al. 2002) extended the nodal analysis approach to be more efficient and faster by reducing the number of equations that describe many MEMS devices. The newly used equations are also based on nodal analysis approach. The proposed procedure was compared with experimental data where a torsional micromirror with lateral actuators and a prototyping of a microrobot were included as illustrative examples. Results showed that the developed package can simulate and synthesis complex MEMS devices, beginning with a high-level description of the device's desired behavior, design objectives and operating constraints. (Zhou et al. 2001) presented a preliminary research on the automatic synthesis of MEMS structures using multi-objective genetic algorithms (MOGAs). The case study was to find an optimal topology of a simple MEMS supporting spring structure (meandering spring); this spring is used to form a MEMS resonator. Genetic Algorithms (GA) is used as a global optimization technique; however, since most engineering problems involve more than one objective function, the MOGAs was applied in this paper of MEMS design. Later on (Zhou et al. 2002) proposed a general architecture for using evolutionary algorithms to achieve MEMS synthesis. The design procedure is iteratively achieved by combining multi-objective genetic algorithms (MOGAs) with a MEMS simulation tool (SUGAR). The algorithm is considering the topology and size of MEMS structures. A meandering MEMS resonator is solved for size and topology optimization; MOGAs generates a Pareto set of 26 optimal designs. Results demonstrated the feasibility of the proposed algorithm.

THEORETICAL BACKGROUND

a) Mechanical Resonators

Mechanical resonators have been used for applications in precision frequency generation, resonant oscillators, and in filters (Mukherrjee et al. 1997). As sensors, silicon resonant micro-sensors have been used for measurement of pressure, acceleration, and vapor concentration (Tang et al. 1990). However, polysilicon micromechanical structures have been electro-statically resonated by means of comb-drives. A comb-drive resonator has been used as an actuator as well as a micro-mechanical filter and it is quite common in MEMS literature. Comb drives for large static displacement have been investigated by (Chen et al. 2004). There is more than one type of mechanical resonators: cantilever resonators and lateral resonators. In this paper we will be concerned with the second type, lateral resonators; however, all resonators yield to the same basic concepts and relations.

1. Mathematical Background and Basic Concepts

Inertial sensing is dependent on the reference frame and what is being measured. Practically speaking, two primary applications define the required reference frames and measurements for most devices: the linear accelerometer and the rotational gyroscope. The accelerometer is generally defined in a Cartesian reference frame and measures the kinematics' force due to a linear acceleration.

Inertial sensor design requires a proof mass (m), an elastic spring, a dashpot, and a method to measure the displacement of the proof mass. On the other hand, in mechanical resonators, the mass is actuated electro-statically using comb-drives that produce electrostatic force generating a displacement on the proof mass. In both inertial sensors and mechanical resonators, the dashpot is usually the volume of air.

2. Lumped-Element Model for a Mechanical Resonator

As mentioned earlier, the main components of a mechanical resonator are a proof mass (m), an elastic spring of stiffness (k), a dashpot of damping coefficient (c) -usually the volume of air- and an actuator that generates a force on the proof mass as shown in figure (1). The differential equation that governs the response of the system represented in (figure 1) can easily be deduced such that:

$$\ddot{x} + 2\zeta\omega_n\dot{x} + \omega_n^2 x = F(t) \tag{1}$$

where ω_n is the natural frequency of the resonator, and ζ is the damping coefficient of the system given by:

$$\omega_n = \sqrt{\frac{k}{m}} \quad and \quad \zeta = \frac{c}{2\omega_n m} = \frac{c}{2\sqrt{km}} \tag{2}$$

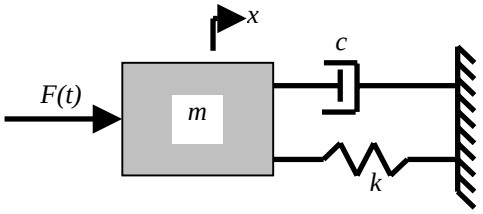

Figure 1. Lumped element model for a microresonator

In mechanical resonators, usually the weight of the shuttle mass is considered when determining the total mass of the resonator, while the mass of the supporting springs can be ignored for approximate analysis. However, if more accuracy is required, in case of folded beam suspension, the following equation by (Kurabayashi, 2004) can be used:

$$m = m_{shuttle} + \tfrac{1}{2} m_{truss} + \tfrac{96}{36} m_{beam} \quad (3)$$

where m_{truss} is the mass of one cross-truss, m_{beam} is the mass of one beam, and $m_{shuttle}$ is the center mass.

The equivalent stiffness (k_{eq}) of the structured resonator has to be determined, in other words if the shuttle mass is supported by more than one spring, the equivalent stiffness that represents those springs must be obtained in order to be modeled as in Figure (1).

b) Electrostatic Comb-Drives

The proof mass of a mechanical resonator is usually actuated using electrostatic comb-drives. The fundamental actuation principle behind electrostatic actuators is the attraction of two oppositely charged plates. Comb-drive type electrostatic micro-actuators make use of large numbers of fingers that are actuated by applying a voltage across them. To generate large forces, large number of fingers is required.

Figure (2) shows a schematic diagram of a comb drive actuator. When the voltage is applied across the movable comb fingers (rotor) and the stationary comb fingers (stator), the rotor moves toward the stator due to an electrostatic force in the *x*-direction. The electrostatic force and the spring balancing force determine the position of the movable fingers (i.e.: the spring stiffness determines the maximum traveling displacement of the rotor). The electrostatic force along the moving direction (*x*-direction) is defined by (Chen et al. 2004):

$$F_{ex} = \frac{N \varepsilon h}{2g} V^2 \quad (4)$$

where N is the number of comb electrode fingers; ε is the permittivity constant of air; h is the comb electrode thickness; g is the comb electrode gap; and V is the driving voltage.

The spring constant (stiffness) in the traveling direction (k_x) and the traveling displacement δ_x, are related as follows:

$$F_{ex} = k_x \,.\, \delta_x \quad (5)$$

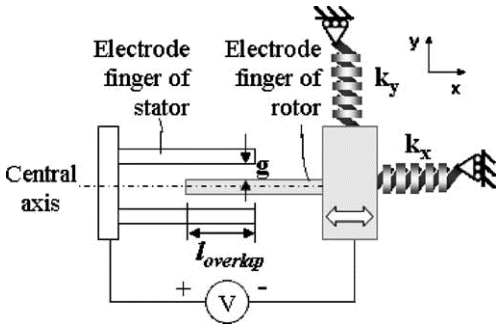

Figure 2. A Schematic diagram of comb drive actuator (Chen et al., 2004)

Substituting into equation (4), one obtains the static actuation displacement such that:

$$\delta_x = \frac{N \varepsilon h}{2k_x g} V^2 \quad (6)$$

THE DEVELOPED HYBRID FUZZY TECHNIQUE

The previously developed optimization techniques of Fuzzy Heuristic Gradient Projection, FHGP, (Senousy et al. 2005) and Heuristic Gradient Projection, HGP, (Metwalli 2004 and Abd El Malek et al. 2005) are effective for shape and geometry optimization. However, they are not that powerful when used for topology optimization. Topological optimization problems involve combinatorial solutions, that is, there is a set of optimal solutions for each problem. Therefore, such optimization problems need further effort in order to select the most appropriate solution. Direct search methods lead to accurate optimal solutions; however, they may be trapped into a local optimum instead of the global optimum. In each iteration, it is therefore desirable to scan the entire solution space to get the accurate global optimum. Random search methods such as genetic algorithms (GA), tabu search (TS), complex method (CM), and simulated annealing (SA) can move iteratively between single solutions or sets of solutions to the global solution. However, they might not be able to find an accurate value for the global optimum solution. In order to solve these difficulties, a combination of both methods (direct methods and random search methods) is a must. In this paper, the Fuzzy Heuristic Gradient Projection (FHGP) -as a local optimization method- is combined with the randomized Complex Method (CM) to get a global optimization method. As a result, the combined method is vigorous and converges to an accurate global optimum in finite time when used for frame topology optimization. In the proposed method, the FHGP method is used for size optimization where elements' dimensions are the only variables and the stress constraints satisfaction is achieved by FHGP as indicated in Senousy et al. (2005). On the other hand, the CM is used for topology optimization where variables are nodes' coordinates and the CM is responsible for satisfying any constraints other than the stress constraints.

1. Complex Method (CM)

The Complex Method (CM) is an extension for the unconstrained minimization simplex method to solve constrained minimization problems (Box, 1965 and Rao 1996) of the type:

$$Minimize \quad f(X) \tag{7a}$$

Subject to:

$$g_j(X) \le 0, \quad j = 1,2,...p \tag{7b}$$

$$x_i^{(l)} \le x_i \le x_i^{(u)}, \quad i = 1,2,...n \tag{7c}$$

Generally, the satisfaction of the side constraints (lower and upper limits for each variable x_i) does not guarantee the satisfaction of the constraints $g_j(X) \le 0$. Since the basic idea of the simplex method is to form a sequence of figures each having $k=n+1$ vertices in an n-dimensional space, in the complex method, a sequence of geometric figures each having $k \ge n+1$ vertices is formed in order to find the constrained minimum point. The complex method cannot be started unless there is a feasible point X_1 that satisfies all the p constraints and all the side constraints.

Iterative Procedure

1. Start with a feasible vertex X_1 that satisfies all the p constraints and all the side constraints.
2. A geometric figure having $k \ge n+1$ is formed such that the starting point is X_1, and the remaining $k-1$ points are found once at a time by using random numbers generated in the range 0 to 1, such that

   $$x_{i,j} = x_i^{(l)} + r_{i,j}(x_i^{(u)} - x_i^{(l)}), \; i = 1,2,..n, \; j = 1,2,..k \tag{8}$$

   where $x_{i,j}$ is the i^{th} component of the point X_j, and $r_{i,j}$ is a random number in the interval (0,1)
3. The generated (X_j, j=2,3,….k) points, generated according to equation (8), satisfy the side constraints, but may not satisfy the constraints $g_j(X) \le 0$. If a point X_j violates any of the constraints stated in equation (7b), the point is to be moved halfway toward the centroid of the remaining, already accepted points (X_o), such that:

   $$X_{j,new} = 0.5(X_o + X_j) \tag{9}$$

   and,

   $$X_o = \frac{1}{j-1}\sum_{l=1}^{j-1} X_l \tag{10}$$
4. If the generated point $X_{j,new}$ still violates any of the constraints, the process of moving toward the centroid is continued until a point that satisfies all the p constraints is obtained. By proceeding this way, a set of k feasible points that satisfy all the p constraints are obtained.
5. The objective function is evaluated at each of the $k \ge n+1$ vertices.
6. The vertex X_h that corresponds to the highest objective function value is reflected to find a new point X_r such that

   $$X_r = (1+\alpha)X_o - \alpha X_h \tag{11}$$

   where α = 1.3 is found to be satisfactory by (Box, 1965), and X_o is the centroid of all vertices except X_h:

   $$X_o = \frac{1}{k-1}\sum_{l=1,l\ne h}^{k} X_l \tag{12}$$
7. The point X_r has to be tested for feasibility:

   7.a. If the point X_r is feasible and $f(X_r) < f(X_h)$, the point X_h is replaced by X_r and we go to step 5.

   7.b. If the point X_r is feasible but $f(X_r) \ge f(X_h)$, a new trial point X_r is found by reducing the value of α by a factor of 2 and the point is tested for the satisfaction of the relation $f(X_r) < f(X_h)$. The process of reducing α is repeated until the relation is satisfied or α becomes smaller than a small quantity 10^{-6}.

   7.c. If an improved point X_r with $f(X_r) < f(X_h)$ cannot be obtained, the point X_r is discarded and the entire procedure of reflection is repeated using the point X_p that has the second-highest objective function value instead of X_h.
8. If the point X_r satisfies the relation $f(X_r) < f(X_h)$ but violates any of the constraints (not feasible), it is moved halfway toward the centroid until it satisfies all the p constraints (becomes feasible), that is,

   $$X_{r,new} = 0.5(X_o + X_r) \tag{13}$$
9. Each time the highest objective function value X_h is replaced by a new point, a check for convergence has to be performed. The process is converged whenever the standard deviation of the function value at the k vertices becomes sufficiently small, that is,

   $$S = \left\{\sum_{i=1}^{k} \frac{[f(X) - f(X_o)]^2}{k}\right\}^{1/2} \le \varepsilon_2 \tag{14}$$

   where X_o is the centroid of all the k vertices of the current complex, and $\varepsilon_2 > 0$ is a specified small number.

Some minor modifications have been introduced to the Complex Method (CM) before it is hybridized with the Fuzzy Heuristic Gradient Projection (FHGP) approach in order to

enhance the performance of the proposed hybrid fuzzy technique.

2. Modifications of the Complex Method (CM)

i) Starting the optimization process using the complex method is mainly dependant upon the starting point, which must be feasible. The initial vertices are completed by randomly creating some points that satisfy all the side constraints. However, as these points might violate some other constraints, the CM suggests moving halfway toward the centroid of the feasibly accepted points. Consequently, the method will progress toward the optimum point as long as the complex has not collapsed into its centroid. In order to solve this problem, the new proposed method suggests that the initialization of all of the vertices is random, that is, if a randomly chosen vertex violates any of the constraints, another vertex is randomly chosen instead of moving toward the centroid of the accepted points. In addition to preventing the complex from collapsing into its centroid, this modification achieves the goal of the random search methods (finding a global optimum), since it scans all the entire design space when choosing its points.

ii) As mentioned above, in the proposed hybrid fuzzy technique, the CM is responsible for selecting the optimum nodes' locations while the FHGP method is responsible for calculating the optimum members' dimensions. However, a vertex is composed of nodes' coordinates in addition to member's dimensions. The new method proposes calculating the members' dimensions that satisfy the stress constraints using FHGP method and neglecting any other constraint, and in the mean time, randomly chosen nodes' coordinates are found. If the selected locations violate the stress constraints, the FHGP method is used as a feedback controller to recalculate the members' dimensions. While if they violate any other constraints, new locations are selected such that they satisfy all constraints. Finding those locations will be random if the target is to initialize the vertices. While if the process is concerned with reflecting the already-accepted vertices, moving toward the centroid is suitable since collapsing into the centroid is not likely to occur.

3. Hybrid Fuzzy Technique Algorithm

Step_1. **Determination of movable nodes** "$i = 1 \rightarrow n$, n= number of nodes"

- Determine the number of nodes that are allowed to move (n)
- Determine the location of each movable node.
- Specify x and y coordinate limits (upper and lower limits) for each of these nodes.

Step_2. **Vertices initiation**

- Determine the number of proposed vertices (i.e.: $k \geq$ 2*(number of nodes))
- Use FHGP to calculate an optimal structural size at the initial proposed topology; hence, the first vertex is obtained.
- For j = 2 to k
  - Randomly select x and y coordinates for each movable node.
  - Use FHGP to calculate an optimal structural size for a randomly selected coordinates.
  - Check the feasibility of the vertex j.
  - If the vertex is not feasible, the process of randomization followed by FHGP is repeated until a feasible vertex j is obtained.
  - Next j.
- At this step a set of "k" feasible topologies are obtained.

Step_3. **Reflection**

- The objective function is evaluated at each of the k vertices.
- The vertex X_h that corresponds to the highest objective function value is reflected to find a new point X_r.
- The vertex X_r should satisfy all the side constraints as well as any other constraint.
- If the vertex X_r violates any of the side constraints, it is moved halfway toward the centroid already accepted vertices.
- If the vertex X_r violates stress constraints, the FHGP method is used to satisfy the stress constraint by changing elements' dimensions.
- If the vertex X_r violates any constraint other than the stress and the side constraints, nodes' coordinates are moved halfway toward the already accepted locations.
- The process of reflection is performed for all of the k vertices.

Step_4. **Convergence Check**

The process is converged whenever the standard deviation of the function value at the "k" vertices becomes sufficiently small or the range of objective function values for all vertices is small. The flow chart of algorithm is shown in figure (3).

CASE STUDY AND RESULTS (A MICRO-ELECTRO-MECHANICAL RESONATOR)

A meandering resonator (figure 4) was previously solved in the literature (Kamalian et al. 2002). The design goal is to have a lowest natural frequency of (93723 rad/s). The resonator is comprised of a center mass connected with four springs comprised of a series of flexible beams. The mass moves horizontally by means of two electrostatic comb-drives.

The same problem will be solved in the present work using the proposed technique. However, the design objective of the problem will be altered to be: minimizing the resonator total weight while satisfying the stress inequality constraint in addition to the frequency equality constraint.

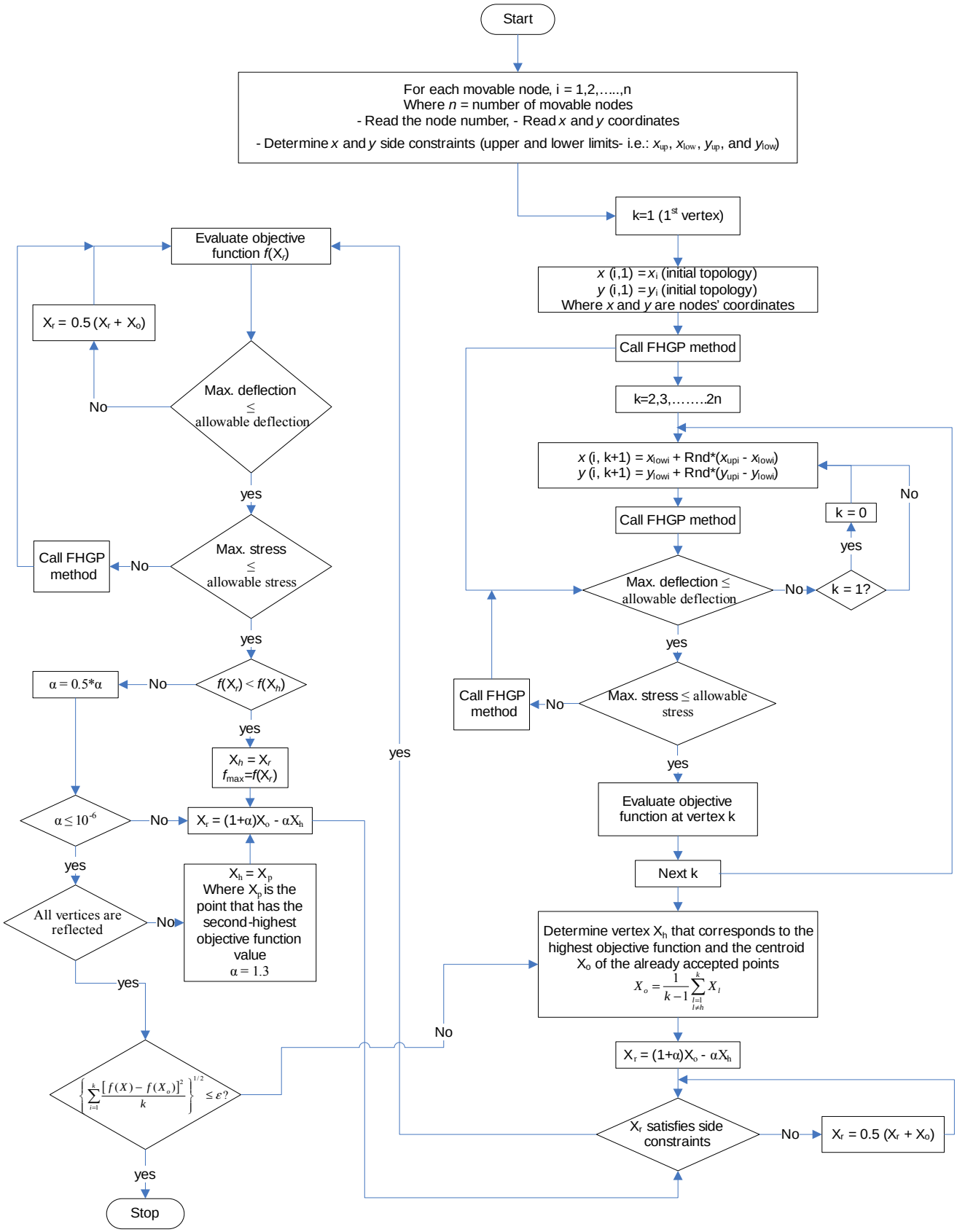

Figure 3. Hybrid Fuzzy Heuristic Gradient Projection method flowchart

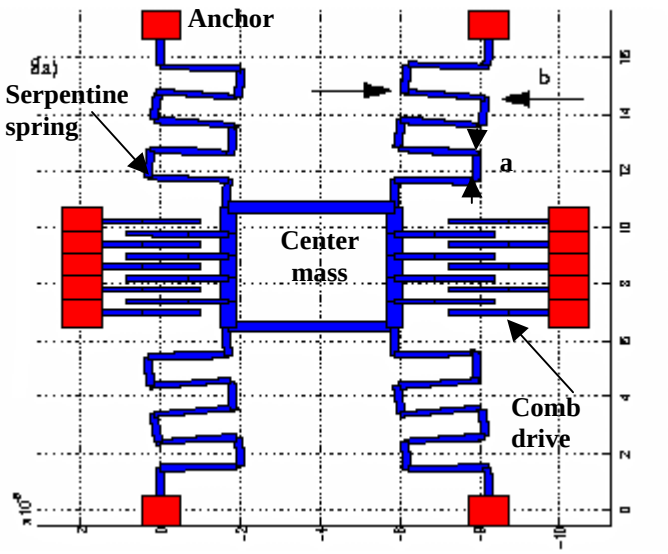

Figure 4. A MEMS resonator with four meandering springs (Kamalian et al. 2002)

1. Problem Formulation

The following equations summarize the objective function as well as the constraints:

$$\text{Minimize} \quad f(X) = \sum_{i=1}^{m} \rho_i w_i l_i t \tag{15}$$

where m is the total number of elements and ρ, w, t, and l are material density, element width, element thickness, and element length respectively.

Subject to:

G_1: Beam thickness (t) = 2 μm;

G_2: Stress constraint $\equiv \sigma_{ti} - S_{uti} \leq 0$

G_3: Frequency constraint $\equiv f$ = 93723 rad/s

G_4: $2 \leq w_i \leq 40$ μm

G_5: Maximum number of beams per leg N_{max} = 7, and minimum number of beams per leg N_{min} = 1

1.1. Design Data

Polysilicon is widely used in the manufacturing of MEMS resonators. Silicon carbide (SiC) and diamond are used in MEMS resonator because of the fact that they can work in harsh environments. In addition, the stiffness of SiC and diamond is quite large, which makes them very attractive for micro-machined resonators and filters, as the resonant frequency increases with increasing the modulus of elasticity (E). The design data for the resonator in hand was taken from an existing resonator that has been fabricated and characterized by (Kamalian et al. 2002).

The design data are as follows:

Polysilicon Material with a Young's modulus (E) of 201 GPa

Material density ρ=2330 kg/m^3

Allowable tensile and compressive stresses (S_{uti}) = 150 MPa

Center mass dimensions (100μm x 100μm x 10μm), (Kamalian et al. 2004)

1.2. Electrostatic Actuation

An electrostatic force is applied to the proof (shuttle) mass using two comb-drives that is subjected to a DC volt = 15V. The specifications of the used comb-drive are listed in (Kamalian et al. 2004) as follows:

Number of electrode comb fingers (N) = 11
Length of comb fingers = 50 μm
Thickness of comb fingers (h) = 4 μm
The comb electrode gap (g) = 3 μm

1.3. Mathematical Model and Assumptions for the Meandering MEMS Resonator

The meandering resonator is comprised of a center mass connected with four springs comprised of a series of beams. In addition, two electrostatic comb-drives are attached to the center mass to actuate the resonator. The electrostatic force produced by the comb drives results in a traveling displacement in the x-direction, while the mass is restricted to move in the y-direction. Since the symmetry of the resonator structure is sought, only one leg of the resonator is considered in the mathematical model when solving for the best topology that achieves the target frequency.

In figure 5, the mass (m) is free to move in the horizontal x-direction, while it is restricted to move in the vertical y-direction. The mass is subjected to electrostatic force produced by the comb drives and can be calculated using equation (4) such that: F_{ex}=14.6 μN

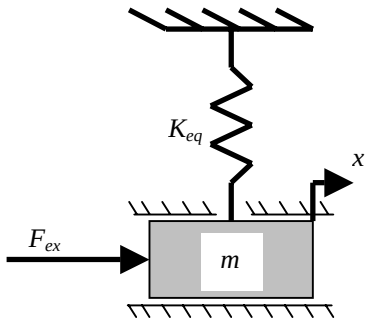

Figure 5. Mathematical model of the resonator

Since the applied electrostatic force is constant and there is an equality frequency constraint, which is a function of the system stiffness and the total mass, the equality frequency constraint can be transformed to be an equality stiffness constraint. That is,

$$\omega_n = \sqrt{\frac{k_x}{m_{shuttle}}} \qquad rad/s$$

where ω_n (required natural frequency) = 93723 (rad/s), and $m_{shuttle}$ is the total weight of the center mass. Hence, the total required stiffness in the x-direction $k_x = 2$ (N/m).

Similarly, since the electrostatic force -which is constant- is a function of the system stiffness and the deflection of the shuttle mass, the equality stiffness constraint can be transformed to an equality deflection constraint.

Substituting into equation 5 or 6, one obtains the maximum lateral displacement $\delta_x = 7.3$ μm.

Since only one spring will be modeled for this problem and the four springs are attached in series, i.e., $K_x = 4K_{eq}$, then applied force is divided by four while the target displacement δ_x is 7.3 (μm) and $K_{eq} = 0.5$ (N/m).

2. Problem Re-formulation

The formulation of the problem is modified to be:

$$\text{Minimize} \quad f(X) = \sum_{i=1}^{m} \rho_i w_i l_i t \qquad (16)$$

where m is the total number of elements and ρ, w, t, and l are material density, element width, element thickness, and element length respectively.

Subject to

G_1: Beam thickness (t) = 2 μm;

G_2: Stress constraint $\equiv \sigma_{ti} - S_{uti} \le 0$

G_3: Deflection equality constraint $\equiv \delta_x = 7.3$ μm

G_4: $2 \le w_i \le 40$ μm

G_5: Maximum number of beams per leg $N_{max} = 7$, and minimum number of beams per leg $N_{min} = 1$

3. Topology Optimization Using the Hybrid Fuzzy HGP Technique

The problem will be solved using the hybrid FHGP technique where the topology is allowed to change within a specified zone. Each node, except the node that is connected to the shuttle mass, is allowed to move in the x and y-directions such that no overlaps occur (figure 6).

The problem has been solved several times; since the proposed hybrid fuzzy technique is based on the random nature of the complex method, it was expected that each time we obtain a final topology that is different from the topology obtained in the previous run. The best four topologies are shown in figure (7).

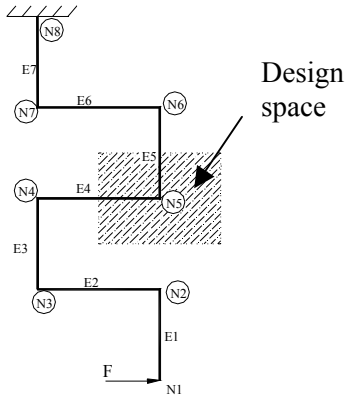

Figure 6. Design space for a MEMS resonator

Table (1) summarizes the objective function value (***OF***), stiffness, frequency, frequency error, and the number of function evaluations (***f Eval***.) for each design alternative (***Sol. No.***).

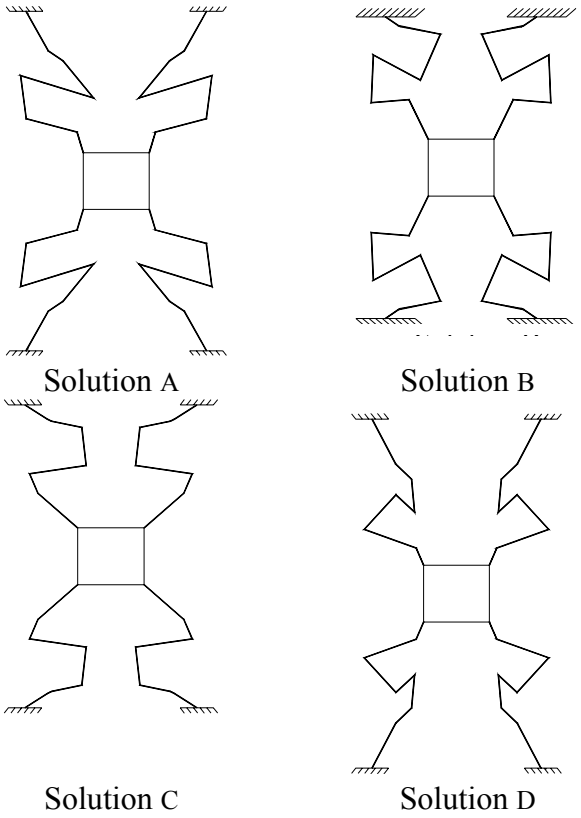

Figure 7. Design alternatives for a MEMS resonator

Table 1. Hybrid FHGP method for a meandering spring resonator

Sol. No.	*Weight* (kg)	*Stiffness* K_x (N/m)	*Freq.* (rad/s)	*Freq. Error %*	*No. of f Eval.*
A	6.54e-12	2.01	93483.31	0.25	39
B	6.02e-12	1.96	92314	1.5	42
C	*4.68e-12*	*2.045*	*94293.71*	*0.60*	*50*
D	5.58e-12	1.922	91414.10	2.46	44

Table 2. Hybrid fuzzy technique for 7-beams spring resonator Stress and Dimensions outputs **(Solution A)**

Element No.	*von-Mises* (MPa)	*Width (w)* (μm)	*Area* $(\mu m)^2$	*OF Weight* (kg)
1	79.90	2.00	4.00	6.54e-12
2	105.02	**8.50**	19.00	
3	9.15	2.00	4.00	
4	18.85	2.00	4.00	
5	74.10	2.13	4.26	
6	81.28	2.00	4.00	
7	150.00	2.86	5.72	

Table 3. Hybrid fuzzy technique for 7-beams spring resonator Nodal displacement **(Solution A)**

Node No.	U_x (μm)	U_y (μm)	K_x (N/m)	*Frequency* (rad/s)	*Error %*
1	**7.263**	00.00	0.5025	$f = \sqrt{\frac{4k_x}{m_{shuttle}}}$ (93483.3)	0.25
2	7.008	-6.589e-2			
3	6.409	-2.019			
4	2.726	-2.433			
5	4.847	3.502			
6	1.806	1.355			
7	1.195	0.579			
8	00.00	00.00			
No. of Function Evaluations			39		

Table 4. Hybrid fuzzy technique for 7-beams spring resonator Stress and Dimensions outputs **(Solution B)**

Element No.	*von-Mises* (MPa)	*Width (w)* (μm)	*Area* $(\mu m)^2$	*OF Weight* (kg)
1	71.92	2.00	4	6.02e-12
2	63.85	2.00	4	
3	57.42	2.00	4	
4	26.60	2.00	4	
5	81.00	4.35	8.70	
6	118.36	2.00	4	
7	150.00	2.74	5.48	

Table 5. Hybrid fuzzy technique for 7-beams spring resonator Nodal displacement **(Solution B)**

Node No.	U_x (μm)	U_y (μm)	K_x (N/m)	**Frequency** (rad/s)	**Error %**
1	**7.462**	00.00	0.4892	(92314)	1.5
2	6.094	-0.579			
3	6.318	-2.962			
4	1.968	-2.801			
5	3.948	0.412			
6	0.456	1.730			
7	0.125	0.158			
8	00.00	00.00			
No. of Function Evaluations				42	

Table 6. Hybrid fuzzy technique for 7-beams spring resonator Stress and Dimensions outputs **(Solution C)**

Element No.	*von-Mises* (MPa)	*Width (w)* (μm)	*Area* $(\mu m)^2$	*OF Weight* (kg)
1	103.65	2.00	4.00	*4.68e-12*
2	77.82	2.00	4.00	
3	27.30	2.00	4.00	
4	6.83	2.00	4.00	
5	90.29	2.00	4.00	
6	108.34	2.00	4.00	
7	150.00	2.72	5.44	

Table 7. Hybrid fuzzy technique for 7-beams spring resonator Nodal displacement **(Solution C)**

Node No.	U_x (μm)	U_y (μm)	K_x (N/m)	*Frequency* (rad/s)	*Error %*
1	**7.140**	00.00	0.51125	$f = \sqrt{\frac{4k_x}{m_{shuttle}}}$ (*94293.71*)	0.60
2	6.482	-0.568			
3	5.906	-1.301			
4	4.487	-1.823			
5	3.801	2.224			
6	0.682	1.920			
7	0.328	0.441			
8	00.00	00.00			

Table 8. Hybrid fuzzy technique for 7-beams spring resonator Stress and Dimensions outputs **(Solution D)**

Element No.	*von-Mises* (MPa)	*Width (w)* (μm)	*Area* $(\mu m)^2$	*OF Weight* (kg)
1	79.62	2.00	4.00	5.58e-12
2	113.76	2.00	4.00	
3	12.28	2.00	4.00	
4	0.40	2.00	4.00	
5	71.30	2.00	4.00	
6	82.54	2.00	4.00	
7	150.00	2.91	5.82	

Table 9. Hybrid fuzzy technique for 7-beams spring resonator Nodal displacement **(Solution D)**

Node No.	U_x (μm)	U_y (μm)	K_x (N/m)	**Frequency** (rad/s)	**Error %**
1	**7.598**	00.00	0.48038	$f = \sqrt{\frac{4k_x}{m_{shuttle}}}$ (91414.10)	2.46
2	7.437	-0.0607			
3	6.669	-1.910			
4	3.771	0.389			
5	5.319	1.841			
6	2.529	1.624			
7	1.487	0.675			
8	00.00	00.00			
No. of Function Evaluations				44	

RESULTS AND DISCUSSION

From the results (Tables 1 to 9) and in figure (8), it can be concluded that *"Solution C"* is the best from the objective function perspective where it achieves the lowest objective function value (4.68e-12 kg). Solution C ranks second among the design alternatives from the frequency point of view as the frequency error is (0.6 %) as shown in figure (9). All members of this design alternative are of equal widths except the element number one; however, the value of its width is somehow near to other elements' widths. On the other hand, the number of function evaluations in *"Solution C"* (Fig. 10), is the highest (50 function evaluations); nevertheless, the time consumed for those function evaluations is near to 20 minutes.

From results in figure (9), it can be concluded that "*Solution A*" is the best from the frequency point of view where the frequency error is (0.25%) while *"Solution C"* is ranked second. The total number of function evaluations for "*Solution A*" is the least; however, "*Solution A*" is rejected as it has the worst objective function value (6.45e-12 kg). In addition, in "*Solution A*", the width of the element number "2" is large compared with the other elements (Table 2) which forces this design alternative to be rejected from the manufacturing point of view.

Figure (10) shows the number of function evaluations for the four obtained design alternatives. The maximum number of function evaluations is 50 (*Solution C*) while the minimum number of function evaluations is 39 (*Solution A*). However, the time consumed for a single run using the proposed hybrid fuzzy technique on a Pentium4 computer is around 25 seconds. Therefore, the number of function evaluations criterion can be discarded when judging which design alternative is the best.

"Solution C" is selected to be the best design alternative. The use of the proposed hybrid fuzzy technique improves the efficiency of the pure fuzzy technique. The objective function value has been improved by a percentage of 25.86 %, from (6.312e-12 kg) to (4.68e-12 kg).

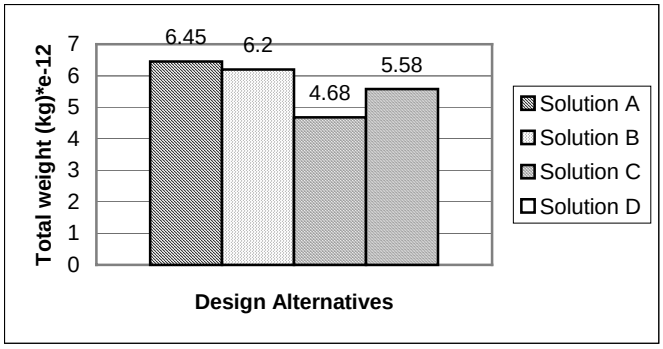

Figure 8. Design alternatives for a MEMS resonator categorized by weight

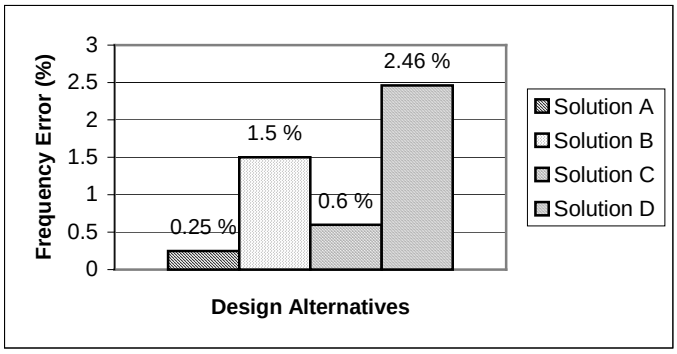

Figure 9. Design alternatives for a MEMS resonator categorized by frequency error %

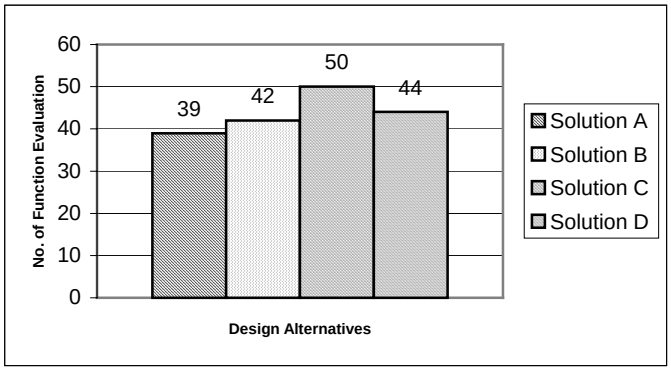

Figure 10. Design alternatives for a MEMS resonator categorized by number of function evaluation

Comparison with Previous Work

The same problem was previously solved in the literature using beam elements and Multi-objective Genetic Algorithms (MOGA) as an optimization technique by (Zhou et al. 2002) as shown in figure (11). It has been stated that a Pareto optimal set of *26* designs was found from one MOGA run. The parameters for one MOGA run are: the population size (n_{pop}) is 400, the number of generations (n_{gen}) is 30, the crossover probability (P_c) is 0.7, the total percentage of elite (P_e) is 5%, and the mutation probability (P_m) is 0.1. The number of function evaluation is *18000* objective function evaluations.

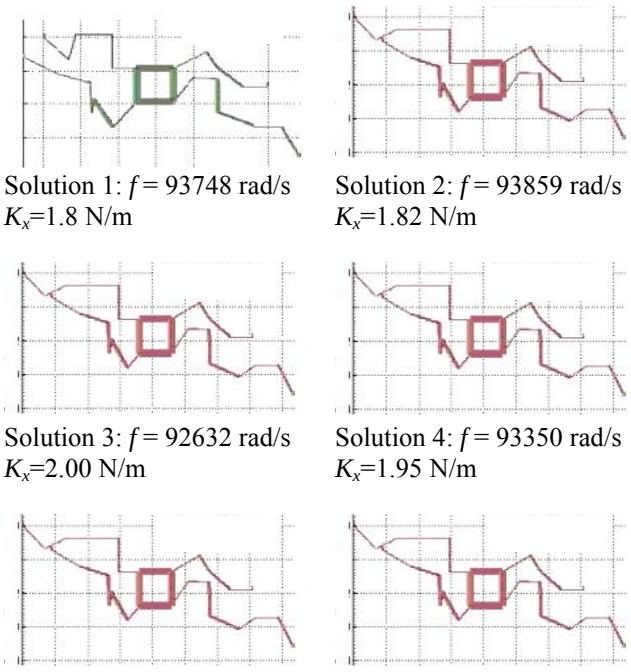

Solution 1: f = 93748 rad/s
K_x=1.8 N/m

Solution 2: f = 93859 rad/s
K_x=1.82 N/m

Solution 3: f = 92632 rad/s
K_x=2.00 N/m

Solution 4: f = 93350 rad/s
K_x=1.95 N/m

Solution 5: f = 94290 rad/s
K_x=1.84 N/m

Solution 6: f = 87368 rad/s
K_x=1.90 N/m

Figure 11. Design examples of meandering resonator (Zhou et al. 2002)

Figure (11) shows some of the 'equally good' Pareto solutions -obtained by (Zhou et al. 2002)- with different configurations, combined with the stiffness and frequency values for each design alternative. It has been stated that the 30 generations took 4-5 hours to complete. When introducing more constraints such that all members must have Manhattan geometry and considering the symmetry, the time consumed was improved to be 1.5 hour. However, the proposed hybrid fuzzy technique took around 20 minutes to obtain an optimal solution. Thus the total time is improved by a percentage of (77%).

CONCLUSION

The current work presented a new methodology for the design and optimization of 3D-frames using linear beam elements. The Complex Method (CM) is hybridized with the Fuzzy Heuristic Gradient Projection (FHGP) optimization technique to produce a global optimization method that is able to find global optimum topologies in a considerably short time. The developed method is used to solve a MEMS resonator for a minimum weight. Results are compared with those obtained using the Multi Objective Genetic Algorithms (MOGAs). The proposed method proves to be faster than the MOGAs as the total time consumed to obtain a global optimum is improved by a 77%.

NOMENCLATURE

a, b	Dimensions
c	Damping coefficient
E	Modulus of elasticity
f	Objective function; frequency
F	Force
g	Constraint function; comb electrode gap
G_1 ,..	Constraints 1, .., p
h	Comb electrode thickness
I	Moment of inertia
i, j, k	Index Number
k	Spring constant
K_x	MEMS equivalent stiffness in x-direction
L	Length
m	Mass
n	Number
N	Number of beams; Node
p	Number of constraints
S	Standard Deviation
S_{ut}	Allowable stress
t	Thickness
U	Displacement
V	Voltage
w	Width
X	Design vector
x, y	Cartesian coordinates
ε	Permittivity constant
δ	Deflection
ρ	Density
σ	Normal stress
ω	Natural Frequency
ζ	Damping Ratio

REFERENCES

[1] Abd El Malek, M.R., Senousy M.S., Hegazi, H.A., Metwalli, S.M., (2005), "Heuristic Gradient Projection for Optimization of 3D Space Frames," Proceedings of ASME International Design Engineering Technical Conference and Computers in Engineering Conference, September 24-28, 2005, Long Beach, California, USA. Paper No. DETC2005-85348.

[2] Chen, C., and Lee, C., (2004), "Design and Modeling for Comb Drive Actuator with Enlarged Static Displacement," Sensors and Actuators, A 115 (2004), 530-539.

[3] Clark, J.V., Bindel, D., Kao, W., Zhu, E., Kuo, A., Zhou, N., Nie, J., Demmel, J., Bai, Z., Govindjee, S., Pister, K.S.J., Gu, M., and Agogino, A., (2002), "Addressing the

needs of Complex MEMS Design," Proceedings of the 15th IEEE International MEMS Conference, pp. 204-209.

[4] Clark,J. V., Zhou, N., Bindel, D., Schenato, L., Wu, W., Demmel, J. and Pister, K. S. J., (2002) "3D MEMS Simulation Modeling Using Modified Nodal Analysis," Proceedings of the Microscale Systems: Mechanics and Measurements Symposium, June 8, 2000, Orlando FL, USA pp. 68-75.

[5] Gad-el-Hak, M., (2002), "The MEMS Handbook," CRC Press LLC.

[6] Kamalian, R., Zohu, N., and Agogino, A.M., (2002), "A Comparison of MEMS Synthesis Techniques", 1st Pacific Rim Workshop on Transducers and Micro/Nano technologies, Xiamen, China, pp 239-242.

[7] Kamliann, R., Agogino, A.M., and Takagi, H., (2004), "The Role of Constraints and Human Interaction in Evolving MEMS Designs: Microresonator Case Study," Proceedings of DETC2004: ASME 2004 Design Engineering Technical Conferences, September 28-October 2, Salt Lake City, Utah, Paper Number DETC04/DAC-57462.

[8] Kamalian, R, Takagi, H. and Agogino, A.M., 2004, "Optimized Design of MEMS by Evolutionary Multi-objective Optimization with Interactive Evolutionary Computation", Proceedings of the 2004 Genetic and Evolutionary Computation Conference, GECCO-2004.

[9] Kurabayashi, k., (winter 2004), "Resonance in MEMS, Lecture notes," Mechanical Engineering, University of Michigan, College of Engineering.

[10] Metwalli, S.M., (1999), "FRAME3D: Computer Aided Design of Space Frames Using Beam Elements," Privately developed program.

[11] Metwalli, S.M., (2004), "Synthesis Paradigm in Computer Aided Design and Optimization of Mechanical Components and Systems," Current Advances in Mechanical Design and Production VIII, Vol. III, Cairo University, pp. 3-11.

[12] Mukherjee, T., and Fedder, G.K., (1997), "Structured Design of MicroElectroMechanical Systems MEMS," DAC'97, Anaheim, California.

[13] Rao, S. S., (1996), "Engineering Optimization, Theory and Practice," Third Edition, A Wiley Interscience Publication, John Wiley & Sons, Inc.

[14] Senousy M.S., Hegazi, H.A., Metwalli, S.M., "Fuzzy Heuristic Gradient Projection for Frame Topology Optimization," (2005), Proceedings of the ASME International Design Engineering Technical Conference and Computers in Engineering Conference, September 24-28, 2005, Long Beach, California, USA. Paper No. DETC2005-85353.

[15] Tang, W.C., Nguyen, T.C.H, and Howe, R.T., (1989), "Laterally Driven Polysilicon Resonant Microstructure," Sensors and Actuators, 20, 41-48.

[16] Tang, W.C., Nguyen, T.C.H, Judy, M.W., and Howe, R.T., (1990), "Electrostatic-comb Drive of Lateral Polysilicon Resonators," Sensors and Actuators, A21-A23 (1990), 323-331.

[17] Varadan, V.K., Jiange, X., and Varadan, V.V., (2001), "Microstereolithography and Other Fabrication Techniques for 3D MEMS", First Edition, John Wiley & Sons Ltd.

[18] Zhou, N., Zhu, B., Agogino, A. M. and Pister, K. S. J., (2001), "Evolutionary Synthesis of MEMS MicroElectronicMechanical Systems Design," Intelligent Engineering System through Artificial Neural Networks Proceedings of the Artificial Neural Networks in Engineering (ANNIE2001), 11, ASME Press, pp.197-202.

[19] Zhou, N., Agogino, A., and Pister, K. S. J., (2002), "Automated Design Synthesis for Micro-Electro-Mechanical Systems (MEMS)," Proceedings of DETC2002: ASME 2002 Design Engineering Technical Conferences and Computers and Information in Engineering Conference, Montreal, Canada, September 29-October 2, Paper Number DETC2002/DAC-34065.

